



Published in final edited form as:

*Chem Commun (Camb)*. 2021 May 11; 57(38): 4678–4681. doi:10.1039/d1cc01245b.

## Small molecule binding to Inhibitor of nuclear factor kappa-B kinase subunit beta in an ATP non-competitive manner

John V. Napoleon<sup>a,†</sup>, Sarbjit Singh<sup>a</sup>, Sandeep Rana<sup>a,†</sup>, Mourad Bendjennat<sup>a,†</sup>, Vikas Kumar<sup>b</sup>, Smitha Kizhake<sup>a</sup>, Nicholas Y. Palermo<sup>b</sup>, Michel M. Ouellette<sup>c,f</sup>, Tom Huxford<sup>d</sup>, Amarnath Natarajan<sup>a,e,f</sup>

<sup>a</sup>Eppley Institute for Research in Cancer and Allied Diseases, UNMC

<sup>b</sup>VCR Core Facility, UNMC

<sup>c</sup>Division of Gastroenterology and Hepatology, Department of Internal Medicine, UNMC

<sup>d</sup>Structural Biochemistry Laboratory, Department of Chemistry & Biochemistry, San Diego State University, San Diego, CA 92182, United States

<sup>e</sup>Department of Pharmaceutical Sciences and Department of Genetics, Cell Biology and Anatomy, UNMC

<sup>f</sup>Fred & Pamela Buffett Cancer Center, University of Nebraska Medical Center, Omaha, Nebraska 68022, United States

### Abstract

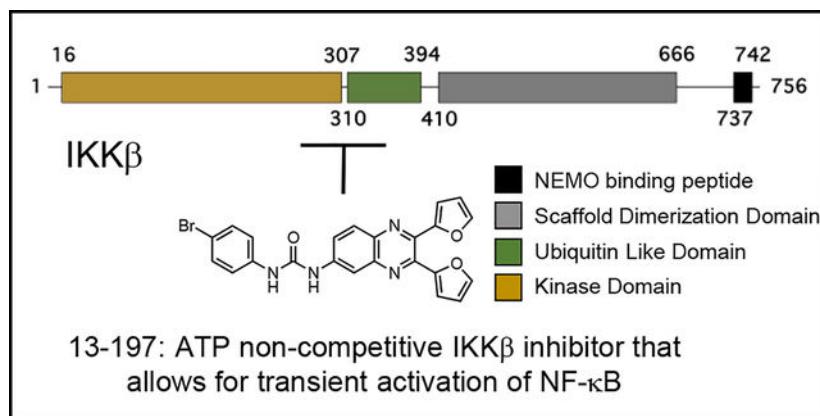
Inhibitor of nuclear factor kappa-B kinase subunit beta (IKK $\beta$ ) is a key regulator of the canonical NF- $\kappa$ B pathway. IKK $\beta$  has been validated as a drug target for pathological conditions, which include chronic inflammatory diseases and cancer. Pharmacological studies revealed that chronic administration of ATP-competitive IKK $\beta$  inhibitors resulted in unexpected toxicity. We previously reported the discovery of 13–197 as a non-toxic IKK $\beta$  inhibitor that reduced tumor growth. Here, we show that 13–197 inhibits IKK $\beta$  in a ATP non-competitive manner and an allosteric pocket at the interface of the kinase and ubiquitin like domains was identified as the potential binding site.

### Graphical Abstract

<sup>†</sup>Current address: JVN (Purdue University, IN), SR (NIH/NCATS, MD), MB (University of Miami, FL)

Electronic Supplementary Information (ESI) available: [details of any supplementary information available should be included here].  
See DOI: 10.1039/x0xx00000x

There are no conflicts of interest to declare



Tumour necrosis factor (TNF)  $\alpha$  has been implicated as a driver of chronic inflammatory diseases (CIDs) and is found in ~50% of the tumour microenvironment of surgically resected tumour samples.<sup>1, 2</sup> TNF $\alpha$  induced IKK $\beta$  phosphorylation results in the activation of the canonical nuclear factor kappa-light-chain-enhancer of activated B cells (NF- $\kappa$ B) pathway.<sup>3</sup> This led to an extensive search for viable IKK $\beta$  inhibitors as CID and cancer therapeutics.<sup>4</sup> A major complication with the use of ATP-competitive IKK $\beta$  inhibitors as therapeutics was elucidated using ML-120B, an ATP-competitive IKK $\beta$  inhibitor developed by Millennium pharmaceuticals, Inc.<sup>5</sup> ML-120B administration led to granulocytosis,<sup>6</sup> and prolonged treatment resulted in increased susceptibility to endotoxin mediated death.<sup>7</sup> Another ATP-competitive IKK $\beta$  inhibitor, TPCA1, developed by GlaxoSmithKline (GSK),<sup>8</sup> exhibited unanticipated toxicity, although it also briefly prolonged the survival of mice with lung cancer.<sup>9</sup> These studies clearly demonstrate that IKK $\beta$  is an attractive therapeutic target, however, the ATP binding site is not optimal for inhibitor design.

IKK $\beta$  is 756 amino acids (aa) in length with aa 16–309 adopting a classical kinase domain (KD), aa 310–404 adopting a ubiquitin-like domain (ULD), and aa 410–664 forming a scaffold dimerization domain (SDD) that has a helical blade structure. To date, only 3 groups have reported the structures of IKK $\beta$  that extend through the SDD.<sup>10–12</sup> The human IKK $\beta$  (pdb id: 4KIK) structure (1–664) is a dimer in which the activation loop (S<sup>177</sup> and S<sup>181</sup>) is phosphorylated in protomer B but not in protomer A.<sup>12</sup> The kinase domains (KD) of the two protomers are otherwise identical suggesting that inhibitors that target the ATP binding site are not likely to distinguish between inactive and active IKK $\beta$ . However, the protomer conformations differ outside the KD, such as a ~120 Å<sup>2</sup> pocket at the KD-SDD interface that is open in protomer B (active IKK $\beta$ ) but partially closed in protomer A (inactive IKK $\beta$ ), which offers unique pockets for the design of selective inhibitors.

We previously reported the discovery of a small molecule, 13–197, that inhibited cancer cell growth by perturbing the levels of the anti-apoptotic protein Mcl1.<sup>13, 14</sup> Subsequently we showed that 13–197 was orally bioavailable, reduced tumour growth and metastasis in an orthotopic pancreatic cancer model, and nearly doubled the median survival of mice in a mantle cell lymphoma model.<sup>15–17</sup> Kinome profiling identified IKK $\beta$  as the target of 13–197, however, 13–197 did not share the toxicity profile of ML-120B or TPCA1.<sup>16, 18</sup> We

hypothesized that the differential toxicity profile of 13–197 was due to a different mechanism of action, i.e., 13–197 is an ATP non-competitive inhibitor.

To test this, we assembled a small panel of IKK $\beta$  inhibitors with different core structures for head-to-head comparison studies with 13–197 (Figure 1A). These include ATP-competitive IKK $\beta$  inhibitors PS-1145 and ML-120B which are  $\beta$ -carboline derivatives,<sup>19</sup> Sc-514 an analogue of TPCA1 with a thiophene-2-carboxamide core,<sup>20</sup> the allosteric IKK $\beta$  inhibitor BMS345541, which is competitive with IKK $\beta$  substrate I $\kappa$ B $\alpha$ ,<sup>21</sup> and the non-selective kinase inhibitor staurosporine.

We screened IKK $\beta$  kinase activity *in vitro* against the panel of IKK $\beta$  inhibitors at two different ATP concentrations (3  $\mu$ M and 270  $\mu$ M) (Figure 1B). We observed ~10-fold loss of inhibitory activity with ATP competitive IKK $\beta$  inhibitors (PS-1145, ML-120B and Sc-514) when the ATP concentration was increased 90-fold in the kinase assay. Under similar conditions, the allosteric inhibitor BMS-345541 fared a little better with ~5-fold loss in inhibition, while the non-selective kinase inhibitor staurosporine was >15-fold less potent at 270 $\mu$ M ATP concentration. Interestingly, with 13–197 we observed only a ~1.7-fold loss of IKK $\beta$  kinase inhibitory activity when the ATP concentration was increased 90-fold (Figure 1B). In a follow up ATP dilution series with the ATP-competitive IKK $\beta$  inhibitor Sc-514 we observed that the curve shifted to the right in a dose-dependent manner with increasing concentrations of ATP (Figure 1C). On the other hand, the IC<sub>50</sub> value of 13–197 remained largely unchanged with increasing concentrations of ATP (Figure 1D). These results strongly suggested that 13–197 functions as an ATP non-competitive IKK $\beta$  inhibitor.

Next, in the presence or absence of 13–197, the progress curves for IKK $\beta$  reactions were linear for up to 2 hours. For the Michaelis-Menten and double reciprocal plots for 13–197 the slopes ( $\mu$ M/min) from the above progress curves were plotted against ATP concentration at indicated 13–197 concentrations (Figure 2A and 2B). In the Michaelis-Menten plot (Figure 2A), the apparent K<sub>m</sub> remained unchanged when 13–197 concentration was increased and in the double reciprocal plot (Figure 2B) the lines converged on the X-axis suggesting that 13–197 was non-competitive with respect to ATP against IKK $\beta$ . In comparison, a similar study with ML-120B showed that the apparent K<sub>m</sub> increased with increasing concentrations of ML-120B in the Michaelis-Menten plot (Figure 2C) and in the double reciprocal plot the lines converged on the Y-axis (Figure 2D) indicating that ML-120B is competitive with respect to ATP against IKK $\beta$ .

To identify the binding site of 13–197 on IKK $\beta$ , we adapted the photoaffinity labelling followed by LC-MS/MS approach reported by the Blagg lab to identify the binding site of Novobiocin on HSP90.<sup>22</sup> We generated analogue 37–290 in which the bromine atom of 13–197 was replaced with an azide that could be cross linked to target proteins upon exposure to UV light (Figure 3A). Upon exposure to UV light, the aromatic carbon atom that is ortho to the azido group on 37–290 is susceptible to nucleophilic attack by the  $\epsilon$ -nitrogen atom on lysine residues in proteins. This results in formation of a 2-amino-azepine ring structure which would yield peptides with a +411 Da signal. Briefly, we incubated IKK $\beta$  (20  $\mu$ g) with 37–290 and one sample was subjected to UV cross linking while the other was used as control. The mixture was then subjected to AspN and trypsin digestion followed by LC-

MS/MS analyses (Supplementary Table 1). We identified 9 peptides in the UV crosslinked sample with a +411 Da adduct (Figure 3B). Remarkably, 4/9 peptides had the +411 Da adduct on K<sup>310</sup> (Figure 3C). A recently reported virtual screen, identified a small molecule inhibitor (analogue 124, Figure S1A) that occupied the allosteric pocket, which is formed by  $\alpha$ -helices from the kinase domain (orange, Figure 3D) and a loop between two  $\beta$  sheets in the ULD (green, Figure 3D), proximal to K<sup>310</sup> in IKK $\beta$ .<sup>23</sup> Consistent with their model, the conformation derived through docking 13–197 using Schrödinger showed that the urea moiety in 13–197 is < 5 Å from the imidazole in His<sup>380</sup> in IKK $\beta$  suggesting potential hydrogen bond interaction (Figure S1B).

An underappreciated fact associated with NF- $\kappa$ B signalling is the number of feedback inhibitory mechanisms that are in place to ensure that NF- $\kappa$ B activation is transient. An obvious manifestation of innate immunity in vertebrates is the activation of an inflammatory response. TNF $\alpha$ -induced IKK $\beta$ - mediated NF- $\kappa$ B activation is a critical signalling pathway that serves as an early inflammatory response. In its latent state, NF- $\kappa$ B is sequestered in the cytoplasm by its endogenous inhibitor I $\kappa$ B $\alpha$ . An array of exogenous stimuli, including TNF $\alpha$ , are known to activate this pathway resulting in the degradation of I $\kappa$ B $\alpha$  and nuclear translocation of NF- $\kappa$ B. Rapid activation of NF- $\kappa$ B mediated gene expression is the cellular response to the stimuli. This results in the resolution of the perceived stress that led to activation of the NF- $\kappa$ B pathway. An early gene that is expressed by NF- $\kappa$ B is its endogenous inhibitor I $\kappa$ B $\alpha$  (under 1h post stimulation), which rapidly dampens the response making the whole process transient. Sustained activation of NF- $\kappa$ B pathway proteins is implicated in a number of disease pathologies including cancer.<sup>24, 25</sup> We hypothesized that inhibitors that allow for transient activation of the NF- $\kappa$ B pathway while blocking the sustained activation would serve as viable therapeutics.

To test this hypothesis, we treated HPNE cells with either DMSO or 13–197 and stimulated both sets with TNF $\alpha$ . This resulted in the rapid phosphorylation and degradation of I $\kappa$ B $\alpha$  in both DMSO and 13–197 treated HPNE cells (Figure 4A, compare lanes at 0, 5, 15 and 30 min). Following degradation, I $\kappa$ B $\alpha$  is re-expressed and is phosphorylated due to the continuous presence of TNF $\alpha$  in the media. Interestingly, at the 60 and 120 min time points post-TNF $\alpha$  stimulation we observed reduced phosphorylation of I $\kappa$ B $\alpha$  in the presence of 13–197 when compared to the control (Figure 4A). We also conducted a dose-response study wherein cells were treated with increasing concentrations of 13–197 and stimulated for either 5 min or 120 min with TNF $\alpha$ . The results summarized in Figure 4B show that 13–197 has very little effect on the levels of I $\kappa$ B $\alpha$  phosphorylation at the 5 min time point but inhibited the phosphorylation at the 120 min time point in a dose-dependent manner. Together these results suggests that 13–197 allows for transient NF- $\kappa$ B activation, but blocks the sustained activation of the canonical NF- $\kappa$ B pathway.

Kras mutation is associated with ~30% of all cancers and previous reports have suggested that Kras mutation activates IKK $\beta$ .<sup>9, 26</sup> Consistently, in Kras mutation driven mouse models concurrent elimination of IKK $\beta$  resulted in reduction of tumour growth and increased survival.<sup>9, 26</sup> On the other hand, constitutive activation (S177E, S181E) of IKK $\beta$  in a Kras mutation-driven model leads to very early onset of tumour growth resulting in a dramatic reduction in survival of mice.<sup>27</sup> To determine if Kras mutation contributes to the activation

of IKK $\beta$ , we subjected lysates from isogenic HPNE cell lines with and without Kras mutation to Western blot analyses (Figure 4C).<sup>28, 29</sup> The results reveal elevated basal phosphorylation of I $\epsilon$ B $\alpha$  indicating constitutive activation of IKK $\beta$  by Kras mutation.

Based on our findings we propose a model for IKK $\beta$  regulation and the putative target of 13–197 (Figure 4D). Briefly, in cancers the presence of TNF $\alpha$  in the tumour microenvironment and/or Kras mutation leads to the rapid activation of IKK $\beta$ . This is characterized by phosphorylation of serine residues 177 and 181 in the activation loop of IKK $\beta$ . Previous reports have shown that pS<sup>177,181</sup>-IKK $\beta$  undergoes autophosphorylation at a stretch of serine residues at the C-terminus over a period of 1–2 h, resulting in a hyperphosphorylated form of IKK $\beta$  with reduced kinase activity.<sup>30</sup> To return to the resting state, hyperphosphorylated IKK $\beta$  associates with phosphatases such as PP5 that will dephosphorylate IKK $\beta$ .<sup>31</sup> If this pathway is continuously stimulated, as in the case of cancer or CID, we posit that the hyperphosphorylated form of IKK $\beta$  will accumulate. Based on our data we propose hyperphosphorylated IKK $\beta$  as the putative target of 13–197 (Figure 4D).

In conclusion, here we report the mechanism of action of a non-toxic IKK $\beta$  inhibitor 13–197. Our studies show that 13–197 is an ATP non-competitive inhibitor of IKK $\beta$ . UV crosslinking using an azido analogue of 13–197 followed by LC-MS/MS implicates an allosteric pocket formed by residues from the kinase and ULD in IKK $\beta$  as the potential binding site of 13–197. In cells, 13–197 allows for the transient activation of the NF- $\kappa$ B pathway while inhibiting sustained activation. Our results provide a viable path forward for development of IKK $\beta$  inhibitors that lack the toxicity observed previously with ATP-competitive compounds.

## Supplementary Material

Refer to Web version on PubMed Central for supplementary material.

## Acknowledgements

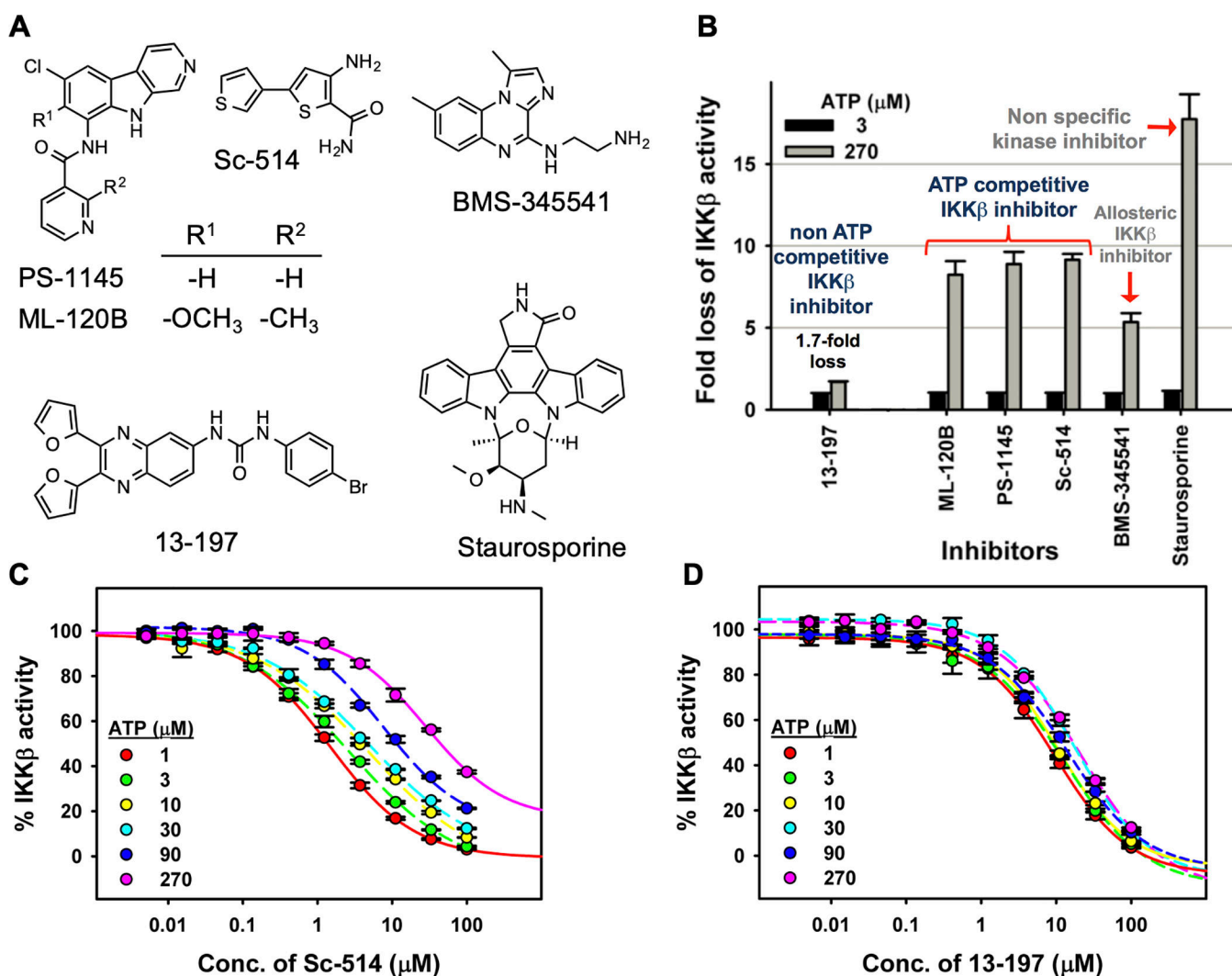
This work was supported in part by NIH grants CA182820, CA197999, CA251151, GM121316 and CA036727. The research resources at UNMC are supported in part by the Nebraska Research Initiative. Biochemistry research at SDSU is supported in part by the California Metabolic Research Foundation. We would like to thank Dr. Koni Stone and the Natarajan lab members for helpful discussions

## References

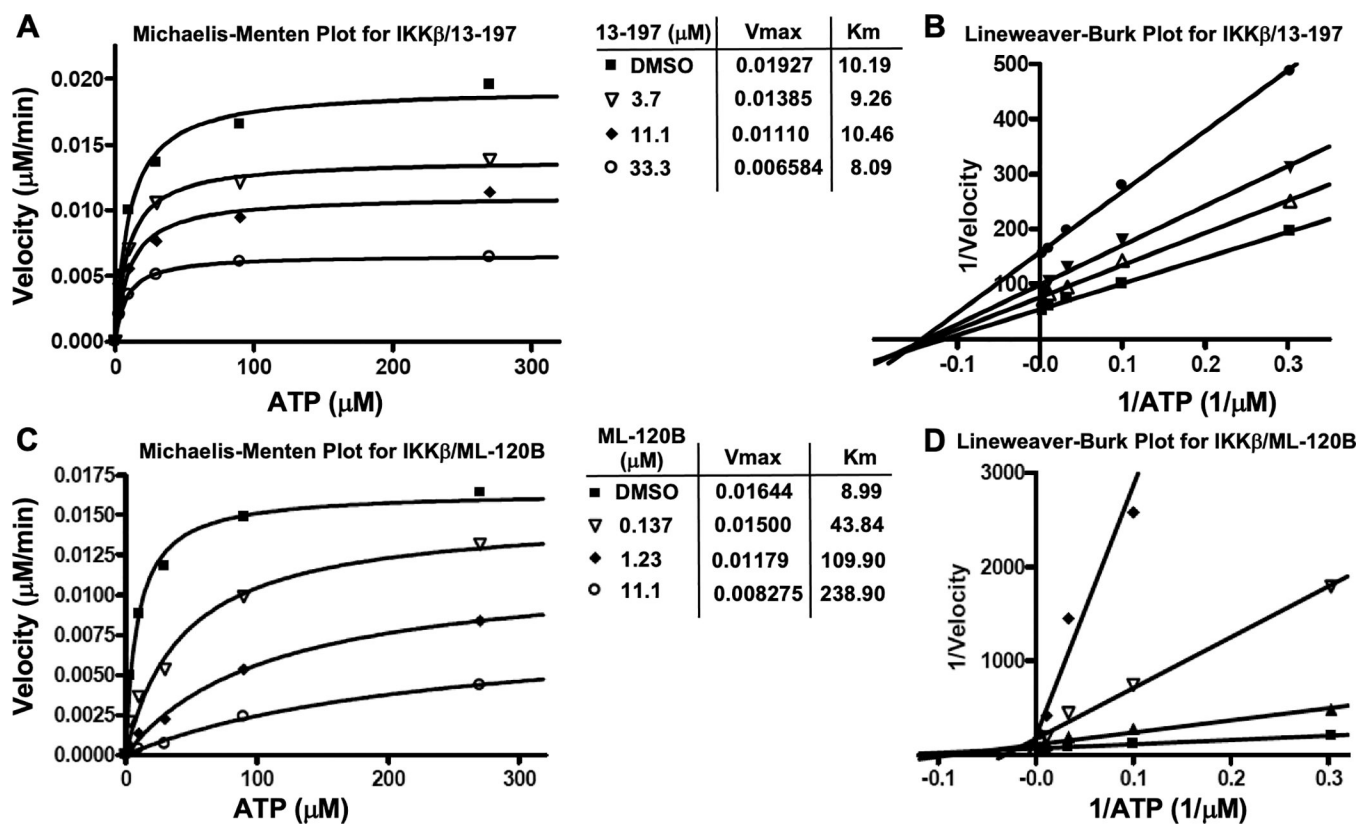
1. Braun J and Sieper J, *Expert Opin Biol Ther*, 2003, 3, 141–168. [PubMed: 12718738]
2. Lee DF, Kuo HP, Chen CT, Hsu JM, Chou CK, Wei Y, Sun HL, Li LY, Ping B, Huang WC, He X, Hung JY, Lai CC, Ding Q, Su JL, Yang JY, Sahin AA, Hortobagyi GN, Tsai FJ, Tsai CH and Hung MC, *Cell*, 2007, 130, 440–455. [PubMed: 17693255]
3. Gilmore TD, *Oncogene*, 2006, 25, 6680–6684. [PubMed: 17072321]
4. Prescott JA and Cook SJ, *Cells*, 2018, 7.
5. Wen D, Nong Y, Morgan JG, Gangurde P, Bielecki A, Dasilva J, Keaveney M, Cheng H, Fraser C, Schopf L, Hepperle M, Harriman G, Jaffee BD, Ocain TD and Xu Y, *J Pharmacol Exp Ther*, 2006, 317, 989–1001. [PubMed: 16525037]
6. Nagashima K, Sasseville VG, Wen D, Bielecki A, Yang H, Simpson C, Grant E, Hepperle M, Harriman G, Jaffee B, Ocain T, Xu Y and Fraser CC, *Blood*, 2006, 107, 4266–4273. [PubMed: 16439676]

7. Greten FR, Arkan MC, Bollrath J, Hsu LC, Goode J, Miething C, Goktuna SI, Neuenhahn M, Fierer J, Paxian S, Van Rooijen N, Xu Y, O’Cain T, Jaffee BB, Busch DH, Duyster J, Schmid RM, Eckmann L and Karin M, *Cell*, 2007, 130, 918–931. [PubMed: 17803913]
8. Podolin PL, Callahan JF, Bolognese BJ, Li YH, Carlson K, Davis TG, Mellor GW, Evans C and Roshak AK, *J Pharmacol Exp Ther*, 2005, 312, 373–381. [PubMed: 15316093]
9. Xia Y, Yedula N, Leblanc M, Ke E, Zhang Y, Oldfield E, Shaw RJ and Verma IM, *Nat Cell Biol*, 2012, 14, 257–265. [PubMed: 22327365]
10. Xu G, Lo YC, Li Q, Napolitano G, Wu X, Jiang X, Dreano M, Karin M and Wu H, *Nature*, 2011, 472, 325–330. [PubMed: 21423167]
11. Polley S, Huang DB, Hauenstein AV, Fusco AJ, Zhong X, Vu D, Schrofelbauer B, Kim Y, Hoffmann A, Verma IM, Ghosh G and Huxford T, *PLoS biology*, 2013, 11, e1001581. [PubMed: 23776406]
12. Liu S, Misquitta YR, Olland A, Johnson MA, Kelleher KS, Kriz R, Lin LL, Stahl M and Mosyak L, *J Biol Chem*, 2013, 288, 22758–22767. [PubMed: 23792959]
13. Chen Q, Bryant VC, Lopez H, Kelly DL, Luo X and Natarajan A, *Bioorg Med Chem Lett*, 2011, 21, 1929–1932. [PubMed: 21376584]
14. Rajule R, Bryant VC, Lopez H, Luo X and Natarajan A, *Bioorg Med Chem*, 2012, 20, 2227–2234. [PubMed: 22386982]
15. Gautam N, Bathena SP, Chen Q, Natarajan A and Alnouti Y, *Biomed Chromatogr*, 2013, 27, 900–909. [PubMed: 23483555]
16. Radhakrishnan P, Bryant VC, Blowers EC, Rajule RN, Gautam N, Anwar MM, Mohr AM, Grandgenett PM, Bunt SK, Arnst JL, Lele SM, Alnouti Y, Hollingsworth MA and Natarajan A, *Clin Cancer Res*, 2013, 19, 2025–2035. [PubMed: 23444213]
17. Chaturvedi NK, Rajule RN, Shukla A, Radhakrishnan P, Todd GL, Natarajan A, Vose JM and Joshi SS, *Mol Cancer Ther*, 2013, 12, 2006–2017. [PubMed: 23963361]
18. Maroni D, Rana S, Mukhopadhyay C, Natarajan A and Naramura M, *Immunol Lett*, 2015, 168, 319–324. [PubMed: 26518140]
19. Hideshima T, Chauhan D, Richardson P, Mitsiades C, Mitsiades N, Hayashi T, Munshi N, Dang L, Castro A, Palombella V, Adams J and Anderson KC, *J Biol Chem*, 2002, 277, 16639–16647. [PubMed: 11872748]
20. Liu Q, Wu H, Chim SM, Zhou L, Zhao J, Feng H, Wei Q, Wang Q, Zheng MH, Tan RX, Gu Q, Xu J, Pavlos N, Tickner J and Xu J, *Biochem Pharmacol*, 2013, 86, 1775–1783. [PubMed: 24091016]
21. Burke JR, Pattoli MA, Gregor KR, Brassil PJ, MacMaster JF, McIntyre KW, Yang X, Iotzova VS, Clarke W, Strnad J, Qiu Y and Zusi FC, *J Biol Chem*, 2003, 278, 1450–1456. [PubMed: 12403772]
22. Matts RL, Dixit A, Peterson LB, Sun L, Voruganti S, Kalyanaraman P, Hartson SD, Verkhivker GM and Blagg BS, *ACS Chem Biol*, 2011, 6, 800–807. [PubMed: 21548602]
23. Liu H, Liang H, Meng H, Deng X, Zhang X and Lai L, *Medchemcomm*, 2018, 9, 239–243. [PubMed: 30108917]
24. Liu F, Xia Y, Parker AS and Verma IM, *Immunol Rev*, 2012, 246, 239–253. [PubMed: 22435559]
25. Baltimore D, *Nat Immunol*, 2011, 12, 683–685. [PubMed: 21772275]
26. Ling J, Kang Y, Zhao R, Xia Q, Lee DF, Chang Z, Li J, Peng B, Fleming JB, Wang H, Liu J, Lemischka IR, Hung MC and Chiao PJ, *Cancer Cell*, 2012, 21, 105–120. [PubMed: 22264792]
27. Naramura M and Natarajan A, *Pancreas*, 2018, 47, e27–e29. [PubMed: 29702533]
28. Lee KM, Nguyen C, Ulrich AB, Pour PM and Ouellette MM, *Biochem Biophys Res Commun*, 2003, 301, 1038–1044. [PubMed: 12589817]
29. Purohit A, Varney M, Rachagani S, Ouellette MM, Batra SK and Singh RK, *Oncotarget*, 2016, 7, 7280–7296. [PubMed: 26771140]
30. Delhase M, Hayakawa M, Chen Y and Karin M, *Science*, 1999, 284, 309–313. [PubMed: 10195894]
31. Chiang CW, Liu WK, Chiang CW and Chou CK, *Biochem J*, 2011, 433, 187–196. [PubMed: 20925653]



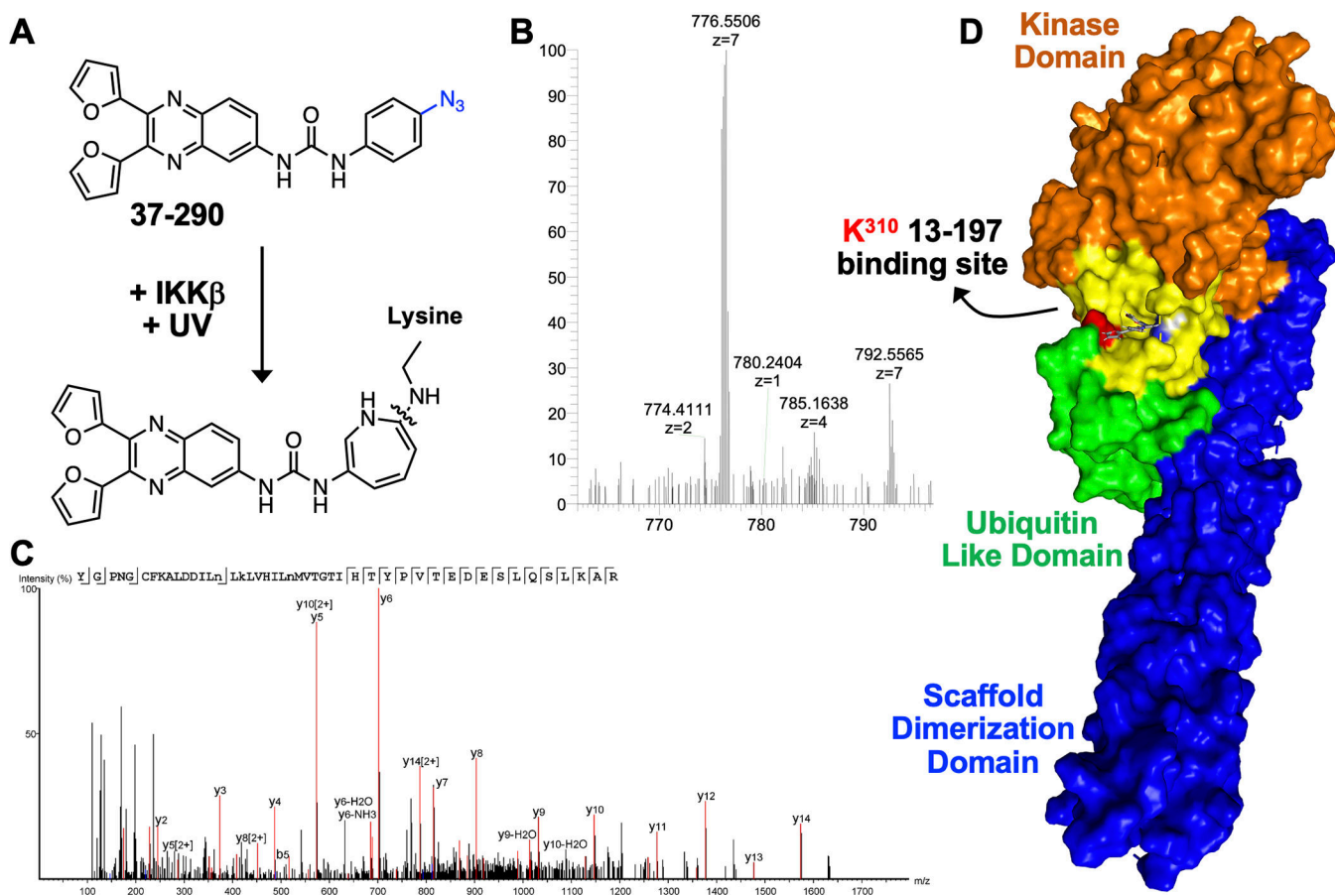


**Figure 1:**  
 (A) Structures of IKK $\beta$  inhibitors. (B) Fold-change in activity of IKK $\beta$  inhibitors due to a 90-fold increase in ATP concentration in *in vitro* IKK $\beta$  kinase assays. (C) Sc-514 dose-response studies with IKK $\beta$  and increasing concentration of ATP. (D) 13-197 dose-response studies with IKK $\beta$  and increasing concentration of ATP.



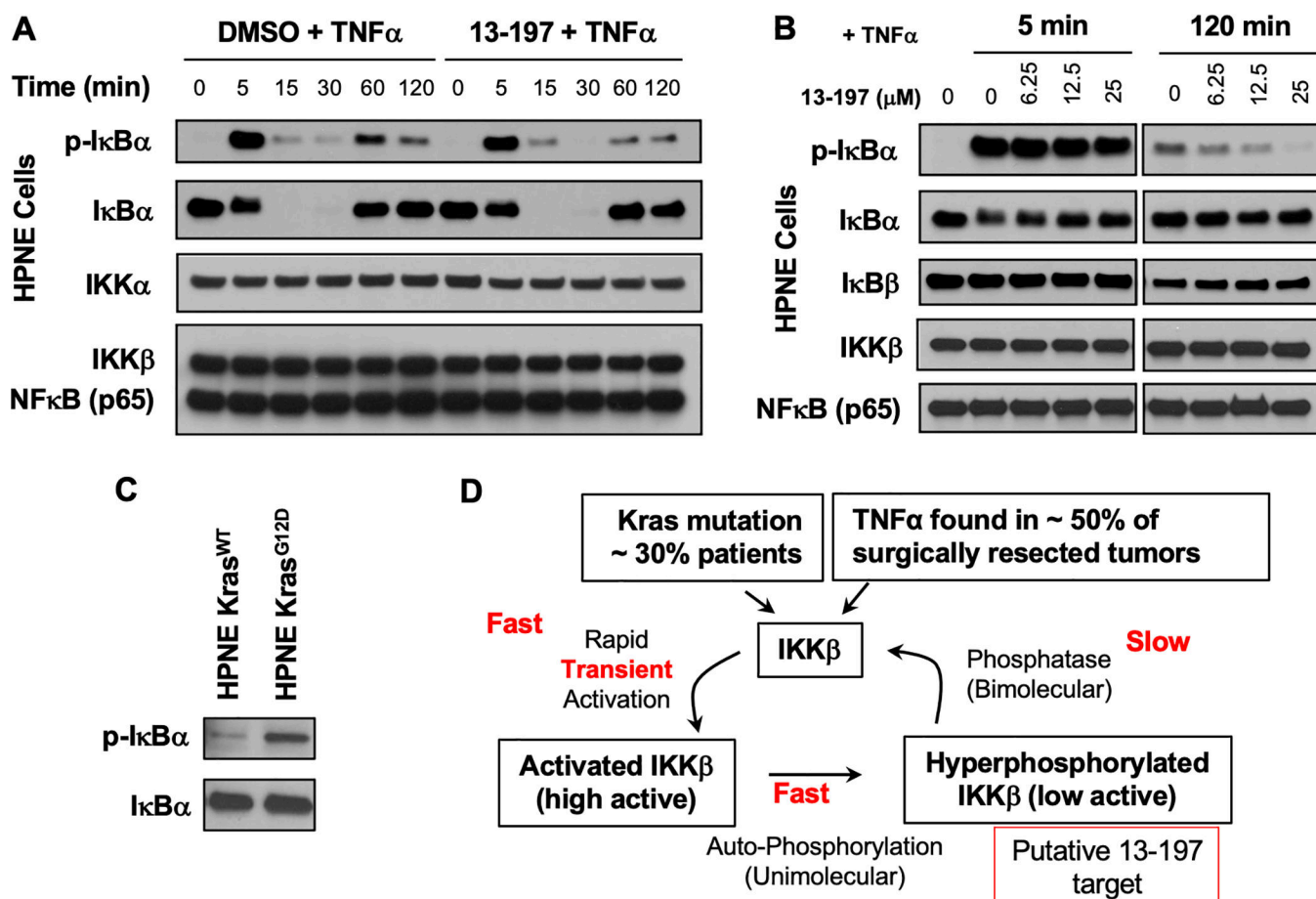
**Figure 2:**  
Michaelis-Menten and double reciprocal plots for IKK $\beta$  with either 13–197 or ML-120B





**Figure 3:**

(A) UV crosslinking 37–290 in the presence of IKK $\beta$  results in the formation of an amino azapine adduct, (B) Representative 37–290 crosslinked mass spectrum. (C) The MS/MS spectrum associated with the 37–290 crosslinked mass spectrum showing the y-ions. (D) Surface rendering of 13–917 docked into the allosteric pocket adjacent to K<sup>310</sup> in IKK $\beta$ .

**Figure 4:**

(A - B) Time course and dose-response studies to assess the effect of 13–197 on TNF $\alpha$  induced activation of IKK $\beta$  mediated I $\kappa$ B $\alpha$  phosphorylation. (C) Basal levels of I $\kappa$ B $\alpha$  phosphorylation in isogenic cell lines with and without KrasG12D mutation. (D) Our model for IKK $\beta$  activation-deactivation and the putative target of 13–197.